arXiv:cond-mat/0008438v1 [cond-mat.mtrl-sci] 30 Aug 2000

Ga^+, In^+ and Tl^+ impurities in alkali halide crystals: distortion trends.

Andrés Aguado
Departamento de Física Teórica, Facultad de Ciencias, Universidad de Valladolid, 47011 Valladolid, Spain
()

A computational study of the doping of alkali halide crystals (AX: A = Na, K; X = Cl, Br) by ns^2 cations (Ga^+, In^+ and Tl^+) is presented. Active clusters of increasing size (from 33 to 177 ions) are considered in order to deal with the large scale distortions induced by the substitutional impurities. Those clusters are embedded in accurate quantum environments representing the surrounding crystalline lattice. The convergence of the distortion results with the size of the active cluster is analyced for some selected impurity systems. The most important conclusion from this study is that distortions along the (100) and (110) crystallographic directions are not independent. Once a reliable cluster model is found, distortion trends as a function of impurity, alkali cation and halide anion are identified and discussed. These trends may be useful when analycing other cation impurities in similar host lattices.

PACS numbers: 61.72.Bb; 61.82.Ms

I. INTRODUCTION

Luminescent materials are used in a wide variety of technological applications.[1] An important proportion of these materials is obtained by doping a pure ionic crystal with substitutional impurities which have desirable absorption-emission properties. The introduction of these substitutional impurities induces a distortion of the host lattice in a local region around the defect, due mainly to the different sizes of the impurity and host ions. That distortion, which is different for each combination of impurity ion and host lattice, determines the specific lattice potential felt by the impurity, and so the location of the impurity electronic levels inside the band gap of the pure crystal. This brief introduction highlights the importance of having a good understanding of the lattice distortions induced by substitutional impurities in ionic crystals. Moreover, their experimental measurement is a difficult task,[2–4] and so theoretical calculations become an ideal complement to the experimental studies.

From the theoretical side, to obtain an accurate characterization of the local structure around a defect is a delicate matter. First of all, the full translational symmetry of the crystal is lost, and so Bloch's theorem can not be directly applied. One way to avoid this problem is to duplicate a finite region of the crystal around the impurity to recover full translational symmetry and exploit the computational convenience of Bloch's theorem. This is done in supercell techniques.[5] The supercell size has to be chosen sufficiently large so that the interaction between the local region influenced by the defect and its periodical images do not interact, because that interaction would be nonphysical. If one forgets about Bloch's theorem, one is left with the cluster approach, in which the doped crystal is modeled by a finite cluster centered on the impurity and embedded in a field representing the rest of the host lattice. This cluster approach is the one chosen in the present study, and has been used in the past to study the geometrical and optical properties of doped crystals.[6–33] In this approach it is important to achieve an accurate description of both the active cluster and the environment. Moreover, those two descriptions should be consistent with each other. Usual deficiencies found in previous works employing the cluster approach are the following: (a) an incomplete representation of the environment. In the simplest and most frequently used approach, the environment is simulated by placing point charges on the lattice sites. This procedure has to be improved in order to obtain a realistic description of the lattice distortions around the impurity.[9–12,15,18,21,24,26,27,31,33] Model potentials have been developed to represent the effects of the environment on the active cluster, that include attractive and repulsive quantum-mechanical terms aside from the classical Madelung term.[34] (b) An active cluster size that is too small. This is usually a problem of the computationally expensive *ab initio* calculations. Only the positions of the ions in the first shell around the impurity are allowed to relax in most cases.[12,24,26,27,29,32] However, geometrical relaxations far beyond the first shell of neighbors can be expected for certain impurities, as suggested by recent semiempirical simulations of solids.[35–43] (c) An abrupt connection between the active cluster and the environment. The wavefunctions and positions of the ions in the environment are not allowed to relax, so that the ions in the surface of the active cluster feel a wrong embedding potential. In previous works,[31,33] we have shown how an unphysically abrupt connection will lead to wrong distortions independently of the intrinsic accuracy of the electronic structure code. (d) An incomplete self-embedding consistency. The cluster model must be tested with calculations on the pure crystals in order to supress systematic errors from the calculated distortions.[31,33]

The most expensive *ab initio* calculations become impractical when the defect induces large-scale lattice dis-

tortions. On the other hand, semiempirical calculations employing pair potentials are not completely reliable due to the problem of transferability to environments different from those in which they were generated. In this paper we employ the *ab initio* Perturbed Ion (aiPI)[44–48]model to study the lattice distortions induced by Ga^+, In^+ and Tl^+ impurities in NaCl, NaBr, KCl and KBr. With the use of this method we circunvent all the incoveniences listed above: (a) The active cluster is embedded in a quantum environment represented by the *ab initio* model potentials of Huzinaga *et al.*[34]; (b) The computational simplicity of the PI model allows for the geometrical relaxation of several coordination shells around the impurity;[15,18,31,33] (c) The local region around the defect in which structural rearrangements are important is connected to the frozen crystalline environment by a smooth interface of ions whose wavefunctions are allowed to selfconsistently relax; (d) Parallel cluster model calculations on the pure crystals are performed in order to obtain trustworthy distortions. By studying several related systems we try to identify systematic distortion trends that might be useful in later theoretical studies of doped crystals similar to those here considered. In a previous publication[33] we considered the case of ns^2 anionic substitutional impurities. Now we complete the study of ns^2 substitutional impurities in alkali halide crystals with a consideration of cationic impurities.

The remainder of this paper is organized as follows: In Section II we describe the active clusters which have been used to model the doped systems. In Section III we present and discuss the results of the calculations, and Section IV summarizes the main conclusions.

II. CLUSTER MODEL

The *ab initio* Perturbed Ion model is a particular application of the theory of electronic separability of Huzinaga and coworkers[49,50] to ionic solids in which the basic building blocks are reduced to single ions. The PI model was first developed for perfect crystals.[44] Its application to the study of impurity centers in ionic crystals has been described in refs. 15,18,31, and we refer to those papers for a full account of the method. In brief, an active cluster containing the impurity is considered, and the Hartree-Fock-Roothaan (HFR) equations[51] for each ion in the active cluster are solved in the field of the other ions. The Fock operator includes, apart from the usual intra-atomic terms, an accurate quantum-mechanical crystal potential and a lattice projection operator which accounts for the energy contribution due to the overlap between the wave functions of the ions.[52] The atomic-like HFR solutions are used to describe the ions in the active cluster in an iterative stepwise procedure. The wave functions of the lattice ions external to the active cluster are taken from a PI calculation for the perfect crystal and are kept frozen during the embedded-cluster calculation. Those wave functions are explicitely considered for ions up to a distance d from the center of the active cluster such that the quantal contribution from the most distant frozen shell to the effective cluster energy is less than 10^{-6} hartree. Ions at distances beyond d contribute to the effective energy of the active cluster just through the long-range Madelung interaction, so they are represented by point charges. At the end of the calculation, the ionic wave functions are selfconsistent within the active cluster and consistent with the frozen description of the rest of the lattice. The intraatomic Coulomb correlation, which is neglected at the Hartree-Fock level, is computed as a correction by using the Coulomb-Hartree-Fock (CHF) model of Clementi.[53,54] The polarization contribution is computed by using the polarizable ion model devised by Madden and coworkers,[55,56] as explained in previous publications.[57,58] In-crystal polarizabilities were obtained from Ref. 59.

Now we describe the cluster models of increasing complexity employed to simulate the impurity systems. All of them are embedded in accurate quantum environments as indicated in the paragraph above. The active clusters are split up into two subsets, which we call $\mathbf{C}_1$ and $\mathbf{C}_2$ following Refs. 15,18. Both the positions and wavefunctions of the ions in the inner $\mathbf{C}_1$ subset are allowed to relax. The positions of the ions in the outer $\mathbf{C}_2$ subset are held fixed during the optimization process, but their wavefunctions are selfconsistently optimized. Thus, the $\mathbf{C}_2$ subset provides a smooth interface connecting the $\mathbf{C}_1$ region, where distortions are important, to the frozen crystalline environment. In practice, $\mathbf{C}_2$ contains all those ions which are first neighbors of the ions in $\mathbf{C}_1$ and are not already contained in $\mathbf{C}_1$. In Table I we show the lattice ions included in the $\mathbf{C}_1$ subset for the different cluster models. It has to be understood that the impurity central ion is included in all cluster models, and that each cluster model is formed by adding the ions shown in Table I to the preceding cluster model. In each case, the geometrical relaxation around the impurity has been performed by allowing for the independent breathing displacements of each shell of ions, and minimizing the total energy with respect to those displacements until the effective energies are converged up to 1 meV. A downhill simplex algorithm[60] was used. For the description of the ions we have used large STO basis sets, all taken from Clementi-Roetti[61] and McLean-McLean[62] tables. The calculations have been performed by employing the experimental lattice constants[63] to describe the geometrically frozen part of the crystals.

The self-embedding consistency of the method has been checked for all the different cluster models and found to be of a quality similar to that found in previous papers.[31,33] By this we mean that if the pure crystal is represented by one of the cluster models enumerated above (that is, if the central impurity is replaced by the alkali cation corresponding to the pure crystal), the results of the cluster model calculations closely agree with those from a PI calculation for the pure crystal, where all

cations (or anions) are equivalent by translational symmetry. Nevertheless, the self-embedding consistency is never complete. In order to supress systematic errors from the distortions calculated with the cluster method, the radial displacements of each shell have been calculated using the following formula:

$$\Delta R_i = R_i(Imp^+ : AX) - R_i(A^+ : AX), \qquad (1)$$

where R_i (i=1, 2, 3, 4, 7, 8) refer to the radii of the first, second, third, fourth, seventh and eigth shells around the impurity in the AX crystal, A = Na, K, X = Cl, Br, and $Imp^+ = Ga^+$, In^+, Tl^+. Thus both systems (pure and doped crystals) are treated in eq. (1) on equal foot so that any inaccuracy in the calculated distortions is completely due to the electronic structure method.

III. RESULTS AND DISCUSSION

A. Influence of the active cluster size

We show in Table II the lattice distortions calculated with the different cluster models described in the previous section, for the NaCl:Tl^+ system. As the distortion trends for different impurity systems will be discussed in the next subsection, here we just point out two general results: (a) the distortion in the first coordination shell, ΔR_1, depends upon an explicit consideration of the distortion in the fourth coordination shell, ΔR_4, that is the distortion along the (100) crystallographic direction propagates at least until next nearest neighbor positions. This is clearly seen in Table II by comparing the value of ΔR_1 in cluster model C with the value of ΔR_1 in cluster models D and E. When the positions of the ions in the fourth coordination shell are held fixed, the ΔR_1 expansion can not attain its optimal value; (b) the distortions along (100) and (110) crystallographic directions are coupled. This means that the calculated distortions in the first and fourth coordination shells depend upon an explicit inclusion of the second and eigth coordination shells in the active clusters. This is seen in the value of ΔR_1 when passing from model A to model B and in ΔR_1 and ΔR_4 when passing from model E to model F. These conclusions are independent of the specific system studied. For example, we show in Fig. 1 the evolution of ΔR_1, as a function of the active cluster complexity, for the three cationic impurities in NaCl. We may appreciate that the three lines are neatly parellel to each other, supporting the validity of our conclusions. Thus, the errors in ΔR_1, due only to a small active cluster size (that is not directly associated with the accuracy of the electronic structure code), can be roughly estimated to be 1%.

A magnitude which is very difficult to estimate theoretically is the defect formation energy. At low pressure and temperature conditions, the formation of the impurity centers should be discussed in terms of the internal energy difference for the exchange reaction[21]

$$(A^+ : AX)_s + Imp_g^+ \rightleftharpoons (Imp^+ : AX)_s + A_g^+, \qquad (2)$$

where the s and g subindexes refer to solid and gas phases, respectively. The Madelung energy term, which is the most important contribution to cohesion in ionic crystals, is minimized when the ions are in their perfect crystallographic positions, so the lattice distortions described above will tend to destabilize this term. The defect will be stable only if the electronic contributions can compensate for that Madelung energy loss. The detailed energy balance contains then nonnegligible contributions from energy terms, like the dispersion interactions, that are not so important for the determination of structural properties. The dispersion interactions, as well as any relativistic energy terms, are not included in the aiPI formalism,[33] so we do not expect the formation energies calculated from it to be wholly reliable. Nevertheless, the contribution to the defect formation energy coming from elastic relaxation of the lattice is meaningful, and we show its evolution as a function of cluster complexity in Fig. 2, for the case of Ga^+, In^+ and Tl^+ impurities in NaCl. Specifically, we show the defect formation *energy differences* (stabilization energies), calculated by substracting the formation energies calculated with a given cluster model and its predecesor. As a reference state for the cluster model A we took a smaller active cluster containing just 7 ions, namely the impurity and its 6 nearest neighbor Cl^- anions, which were held fixed at their lattice positions. This cluster can be considered the limit case of those shown in the previous section, where the $\mathbf{C}_1$ subset is formed by the impurity cation and the $\mathbf{C}_2$ subset (the interphase) is formed just by the six first neighbors of the impurity. The figure seems to suggest that the first shell distortions sligtly destabilize the defects, while second shell distortions largely stabilize them. This apparently paradoxical result is just a consequence of our stepped construction of cluster models. If we include the second shell distortions alone, the net effect is also a destabilization. This simply shows that the distortions in the first and second shells, where short-range overlap interactions with the impurity are important, should be included together in the calculation. Structural relaxation of those two shells provide the largest contribution to elastic relaxation. We also appreciate nonnegligible stabilization energies when the third, fourth, and eigth coordination shells are allowed to relax, giving an idea of the difficulty of obtaining well converged theoretical formation energies.

B. Distortion trends

In this section we show the calculated distortions induced by substitutional Ga^+, In^+ and Tl^+ impurities in NaCl, NaBr, KCl and KBr crystals. For all these calculations we employ the cluster model F, which is the most complete one from those considered in previous sections. These distortions, collected in Table III, are the main

quantitative result from our study. From that table we can extract interesting distortion trends, that we describe in the following:

First shell distortion. This shell undergoes an expansion in all cases, with the only exception of the Ga^+ impurity in K salts. In a previous publication[33] we showed how these distortions can be rationalized in terms of simple geometric arguments involving ion sizes. As a rough measure of ion size we employed the quantity r $= (< r^2 >)^{1/2}$, where the expectation value is taken over the outermost orbital of the ion, and is calculated from the crystal-consistent ionic wave functions obtained through the aiPI calculations. Then the first shell distortions were shown to be related to the differences δ =r(Imp^+:AX)-r(A^+:AX), where r(Imp^+:AX) is the radius of the Ga^+, In^+ or Tl^+ impurities in the AX crystal, and r(A^+:AX) is the radius of the alkali cation in the pure AX crystal. A similar analysis here shows that δ is negative only for KCl:Ga^+ and KBr:Ga^+, giving an explanation to the inwards relaxation of the first shell in those two cases. More in general, for a fixed crystal δ increases in the series $Ga^+ \rightarrow In^+ \rightarrow Tl^+$, as should be expected. The ΔR_1 distortions for any given crystal follow the same trend. For a given impurity and fixed halide anion, the first shell expansion is larger the smaller the size of the alkali cation. This trend suggests what kind of distortions can be expected in Li or Rb host lattices. For example, one can expect a small inwards relaxation for RbCl:In^+, similar to that found for KCl:Ga^+, and more important distortions for Li salts, that perhaps will ask for larger active cluster sizes. For those systems where an expansion is observed, if we fixed the impurity cation and the alkali cation, the expansion is larger the larger the size of the anion. Thus one can expect smaller expansions for NaF and KF salts and larger ones for NaI and KI salts. For those cases where a contraction is observed, the contraction is larger the smaller the size of the anion.

Second shell distortion. The displacement of the second shell is always an expansion. For any given host lattice, that expansion is larger the larger the impurity size, because of the increase in cation-cation overlap repulsion. If the impurity and the halide anion are fixed, the expansion increases with decreasing alkali size. This trend suggests again larger ΔR_2 expansions in Li salts and smaller ones in Rb salts. If the impurity and the alkali cation are fixed, the expansion is larger the smaller the anion size, because cation-cation overlap decreases with increasing anion size. Then, larger ΔR_2 expansions are expected in NaF and KF salts and smaller ones for NaI and KI salts.

Third shell distortion. This shell experiences a small contraction in all cases. For a given crystal, the contraction is larger the larger the size of the impurity. If we fix the impurity and the halide anion, the contraction increases with decreasing alkali size. Then, larger contractions should be expected in Li salts, and smaller ones in Rb salts. If the impurity and the alkali cation are fixed, the contraction is larger the smaller the size of the halide anion, so larger contractions are expected for fluoride salts. As the direct overlap interactions between the impurity and the ions in the third coordination shell are negligibly small, this contraction has to be considered an indirect doping effect, mediated by the distortions induced on the first and second shells. The small contraction of the third shell optimizes the Madelung energy around the impurity and also serves to pack more efficiently the ions in response to the outward motion of the ions in the first and second shells.

Fourth and seventh shell distortions. The fourth shell experiences an expansion, except in the case of KCl:Ga^+. The ΔR_4 displacements proceed along the same (100) crystallographic direction as the ΔR_1 displacements, and thus are clearly induced by the first shell distortions, as indicated in the previous subsection. The distortion trends of this shell are then found to be the same as those of the first shell. The displacements of those ions in the seventh coordination shell are always negligibly small, indicating that the distortions propagate along the (100) direction just until next-nearest neighbor positions.

Eigth shell distortion. Similarly to the previous paragraph, the eigth shell undergoes an expansion induced by the expansion of the second shell, as both displacements proceed along the (110) crystallographic directions. Thus the distortion trends are the same as those found for the second shell.

IV. SUMMARY

A study of the local lattice distortions induced by substitutional Ga^+, In^+ and Tl^+ impurities in NaCl, NaBr, KCl and KBr crystals has been reported. For that purpose we have considered active clusters of increasing complexity, with a number of ions varying between 33 and 177 ions, embedded in accurate quantum environments representing the rest of the crystal. The local distortions obtained extend beyond the first shell of neighbors in all cases. Thus, the assumptions frequently employed in impurity calculations, which consider the active space as formed by the central impurity plus its first coordination shell only, should be taken with some care. Moreover, we have found that the distortions along the (100) and (110) crystallographic directions are not independent from each other, and also that the first shell distortion is not converged if the positions of the ions in the fourth coordination shell around the impurity are not allowed to relax. Once we have obtained a reliable cluster model, distortion trends have been identified and discussed. In those cases where the size of the impurity is larger than that of the alkali cation, the impurity induces an expansion propagating along (100) and (110) crystallographic directions until next-nearest neighbor positions. There is also an indirect contraction along the (111) crystallographic direction, that probably affects only to the nearest neighbor ions in that direction, and which serves to

partly compensate the Madelung field around the impurity and to pack more efficiently the ions in response to the outward motion of the first and second shells. In those cases where the size of the impurity is smaller than that of the alkali cation of the host lattice, the only significant change in these trends is the inwards relaxation along the (100) direction. The dependence of the several shell distortions upon a change of alkali cation, halide anion, and impurity cation have been described. From this description one can advance expected distortions for closely related systems.

Acknowledgements: Work supported by DGES (PB98-0345) and Junta de Castilla y León (VA28/99). The author is greatly indebted to Angel Martín Pendás and Miguel Alvarez Blanco for providing him with an improved version of the aiPI fortran code.

Captions of Tables

Table I. Description of the lattice ions included in the $\mathbf{C}_1$ subset for the different cluster models. The degeneracy (number of symmetry equivalent ions) of each coordination shell is shown, together with the charge of the ions forming that shell, and the total number of atoms in the active cluster (ions in $\mathbf{C}_1$ and $\mathbf{C}_2$ subsets).

Table II. Lattice distortions (in Å) and percentage distortion values obtained with the different cluster models described in the text.

Table III. Lattice distortions (in Å) of several coordination shells around Ga^+, In^+ and Tl^+ impurities in four alkali halide crystals, employing cluster model F as described in the text.

Captions of Figures

Figure 1. First-shell distortions (in Å) induced by Ga^+, In^+ and Tl^+ impurities in NaCl, as a function of the complexity of the cluster model. Note the similar behavior of the three curves.

Figure 2. Defect formation energy stabilization (in eV) as a function of cluster complexity.

[1] G. Blasse and B. C. Grabmaier, *Luminescent materials*, Springer Verlag, Berlin (1995).
[2] J. H. Barkyoumb and A. N. Mansour, Phys. Rev. B **46**, 8768 (1992).
[3] W. F. Pong, R. A. Mayanovic, B. A. Bunker, J. K. Furdyna, and U. Debska, Phys. Rev. B **41**, 8440 (1990).
[4] C. Zaldo, C. Prieto, H. Dexpert, and P. Fessler, J. Phys.: Condens. Matter **3**, 4135 (1991).
[5] M. J. Puska, S. Pöykkö, M. Pesola, and R. M. Nieminen, Phys. Rev. B **58**, 1318 (1998).
[6] H. Chermette and C. Pedrini, J. Chem. Phys. **75**, 1869 (1981).
[7] N. W. Winter, R. M. Pitzer, and D. K. Temple, J. Chem. Phys. **86**, 3549 (1987).
[8] A. B. Kunz and J. M. Vail, Phys. Rev. B **38**, 1058 (1988).
[9] Z. Barandiarán and L. Seijo, J. Chem. Phys. **89**, 5739 (1988).
[10] V. Luaña and L. Pueyo, Phys. Rev. B **39**, 11093 (1989).
[11] V. Luaña, M. Bermejo, M. Flórez, J. M. Recio, and L. Pueyo, J. Chem. Phys. **90**, 6409 (1989).
[12] L. Seijo and Z. Barandiarán, J. Chem. Phys. **94**, 8158 (1991).
[13] J. Andriessen, P. Dorenbos, and C. W. E. van Eijk, Mol. Phys. **74**, 535 (1991).
[14] M. S. Islam and R. C. Baetzold, J. Phys. Chem. Solids **53**, 1105 (1992).
[15] V. Luaña and M. Flórez, J. Chem. Phys. **97**, 6544 (1992).
[16] E. Miyoshi and S. Huzinaga, Phys. Rev. B **48**, 8583 (1993).
[17] A. Scacco, S. Fioravanti, M. Missori, U. M. Grassano, A. Luci, M. Palummo, E. Giovenale, and N. Zema, J. Phys. Chem. Solids **54**, 1035 (1993).
[18] V. Luaña, M. Flórez, and L. Pueyo, J. Chem. Phys. **99**, 7970 (1993).
[19] R. Visser, J. Andriessen, P. Dorenbos, and C. W. E. van Eijk, J. Phys.: Condens. Matter **5**, 5887 (1993).
[20] J. Andrés, A. Beltrán, S. Bohm, A. Flores-Riveros, J. A. Igualada, V. Luaña, A. Martín Pendás, and G. Monrós, J. Phys. Chem. **97**, 2555 (1993).
[21] M. Flórez, M. A. Blanco, V. Luaña, and L. Pueyo, Phys. Rev. B **49**, 69 (1994).
[22] A. Beltrán, A. Flores-Riveros, J. Andrés, V. Luaña, and A. Martín Pendás, J. Phys. Chem. **98**, 7741 (1994).
[23] M. Berrondo and J. F. Rivas-Silva, Int. J. Quantum Chem. Quantum. Chem. Symp. **29**, 253 (1995).
[24] J. L. Pascual and L. Seijo, J. Chem. Phys. **102**, 5368 (1995).
[25] T. J. Gryk and R. H. Bartram, J. Phys. Chem. Solids **56**, 863 (1995).
[26] R. Llusar, M. Casarrubios, Z. Barandiarán, and L. Seijo, J. Chem. Phys. **105**, 5321 (1996).
[27] L. Seijo and Z. Barandiarán, Int. J. Quantum Chem. **60**, 617 (1996).
[28] M. Berrondo, F. Rivas-Silva, and J. B. Czirr, *Proceedings of the International Conference on Inorganic Sintillators and their Applications, SCINT95*. Delft University Press (1996), p. 144.
[29] M. Berrondo and F. Rivas-Silva, Int. J. Quantum Chem. **57**, 1115 (1996).
[30] J. F. Rivas-Silva, A. Flores-Riveros, A. Ayuela, and M. Berrondo, Computational Materials Science **11**, 150 (1998).
[31] A. Aguado, A. Ayuela, J. M. López, and J. A. Alonso, Phys. Rev. B **58**, 11964 (1998).
[32] M. T. Barriuso, J. A. Aramburu, and M. Moreno, J. Phys.: Condens. Matter **11**, L525 (1999).
[33] A. Aguado, J. M. López, and J. A. Alonso, Phys. Rev. B (in press).
[34] S.Huzinaga, L. Seijo, Z. Barandiarán, and M. Klobukowski, J. Chem. Phys. **86**, 2132 (1987).
[35] X. Zhang and C. R. A. Catlow, Phys. Rev. B **47**, 5315

(1993).
[36] X. Zhang, C. K. Ong, and A. M. Stoneham, J. Phys.: Condens. Matter **6**, 5647 (1994).
[37] M. S. Islam and R. C. Baetzold, J. Mater. Chem. **4**, 299 (1994).
[38] M. S. Islam and L. J. Winch, Phys. Rev. B **52**, 10510 (1995).
[39] D. C. Sayle, C. R. A. Catlow, M. -A. Perrin, and P. Nortier, J. Phys. Chem. Solids **56**, 799 (1995).
[40] M. J. Akhtar, Z. D. N. Akhtar, R. A. Jackson, and C. R. A. Catlow, J. Am. Chem. Soc. **78**, 421 (1995).
[41] M. Exner, H. Donnerberg, C. R. A. Catlow, and O. F. Schirmer, Phys. Rev. B **52**, 3930 (1995).
[42] C. R. A. Catlow, M. S. Islam, and X. Zhang, J. Phys.: Condens. Matter **10**, L49 (1998).
[43] C. R. A. Catlow and P. D. Townsend, *Point Defects in Materials*, Academic Press, London (1998).
[44] V. Luaña and L. Pueyo, Phys. Rev. B **41**, 3800 (1990).
[45] V. Luaña, J. M. Recio, and L. Pueyo, Phys. Rev. B **42**, 1791 (1990).
[46] L. Pueyo, V. Luaña, M. Flórez, and E. Francisco, in *Structure, Interactions and Reactivity*, edited by S. Fraga (Elsevier, Amsterdam, 1992), vol. B, p. 504
[47] V. Luaña, M. Flórez, E. Francisco, A. Martín Pendás, J. M. Recio, M. Bermejo, and L. Pueyo, in *Cluster Models for Surface and Bulk Phenomena*, edited by G. Pacchioni, P. S. Bagus and F. Parmigiani (Plenum, New York, 1992), p. 605
[48] V. Luaña, A. Martín Pendás, J. M. Recio, and E. Francisco, Comput. Phys. Commun. **77**, 107 (1993).
[49] S. Huzinaga and A. P. Cantu, J. Chem. Phys. **55**, 5543 (1971).
[50] S. Huzinaga, D. McWilliams, and A. A. Cantu, Adv. Quantum Chem. **7**, 183 (1973).
[51] C. C. J. Roothaan and P. S. Bagus, *Methods in Computational Physics*, vol. 2, 47 (Academic, New York, 1963).
[52] E. Francisco, A. Martín Pendás, and W. H. Adams, J. Chem. Phys. **97**, 6504 (1992).
[53] E. Clementi, IBM J. Res. Dev. **9**, 2 (1965).
[54] S. J. Chakravorty and E. Clementi, Phys. Rev. A **39**, 2290 (1989).
[55] P. A. Madden and M. Wilson, Chem. Soc. Rev. **25**, 399 (1996).
[56] P. J̈emmer, M. Wilson, P. A. Madden, and P. W. Fowler, J. Chem. Phys. **111**, 2038 (1999).
[57] A. Aguado, F. López-Gejo, and J. M. López, J. Chem. Phys. **110**, 4788 (1999).
[58] A. Aguado and J. M. López, (to be published).
[59] P. W. Fowler and N. C. Pyper, Proc. R. Soc. Lond. A **398**, 377 (1985).
[60] W. H. Press and S. A. Teukolsky, Computers in Physics **5**, 426, (1991).
[61] E. Clementi and C. Roetti, At. Data and Nuc. Data Tables **14**, 177 (1974).
[62] A. D. McLean and R. S. McLean, At. Data and Nuc. Data Tables **26**, 197 (1981).
[63] N. M. Ashcroft and N. D. Mermin, *Solid State Physics* (Holt, Rinehart and Winston, New York, 1976).

[

Cluster Model	Lattice site	Degeneracy	Charge	N
A	$(\frac{1}{2},0,0)$	6	-	33
B	$(\frac{1}{2},\frac{1}{2},0)$	12	+	57
C	$(\frac{1}{2},\frac{1}{2},\frac{1}{2})$	8	-	81
D	(1,0,0)	6	+	87
E	$(\frac{3}{2},0,0)$	6	-	117
F	(1,1,0)	12	+	177

Cluster model	ΔR_1	ΔR_2	ΔR_3	ΔR_4	ΔR_7	ΔR_8
A	0.165	–	–	–	–	–
	5.96%	–	–	–	–	–
B	0.152	0.092	–	–	–	–
	5.40%	2.27%	–	–	–	–
C	0.154	0.083	-0.063	–	–	–
	5.49%	2.08%	-1.31%	–	–	–
D	0.174	0.081	-0.058	0.053	–	–
	6.23%	2.03%	-1.20%	0.93%	–	–
E	0.175	0.080	-0.060	0.054	0.006	–
	6.27%	2.00%	-1.25%	0.95%	0.07%	–
F	0.155	0.087	-0.064	0.048	0.004	0.031
	5.52%	2.18%	-1.33%	0.84%	0.04%	0.38%

NaCl	Ga^+	In^+	Tl^+	NaBr	Ga^+	In^+	Tl^+
ΔR_1	0.086	0.136	0.155	ΔR_1	0.094	0.145	0.167
ΔR_2	0.058	0.085	0.090	ΔR_2	0.045	0.068	0.072
ΔR_3	-0.041	-0.061	-0.064	ΔR_3	-0.033	-0.045	-0.051
ΔR_4	0.025	0.043	0.048	ΔR_4	0.028	0.047	0.057
ΔR_7	-0.001	–	0.004	ΔR_7	-0.006	0.005	0.007
ΔR_8	0.021	0.031	0.033	ΔR_8	0.015	0.023	0.024
KCl	Ga^+	In^+	Tl^+	KBr	Ga^+	In^+	Tl^+
ΔR_1	-0.019	0.055	0.066	ΔR_1	-0.012	0.064	0.078
ΔR_2	0.009	0.032	0.039	ΔR_2	0.004	0.025	0.033
ΔR_3	-0.016	-0.033	-0.035	ΔR_3	-0.009	-0.024	-0.029
ΔR_4	-0.007	0.020	0.022	ΔR_4	–	0.023	0.024
ΔR_7	-0.007	–	–	ΔR_7	-0.006	0.003	0.006
ΔR_8	0.007	0.015	0.016	ΔR_8	0.003	0.009	0.010

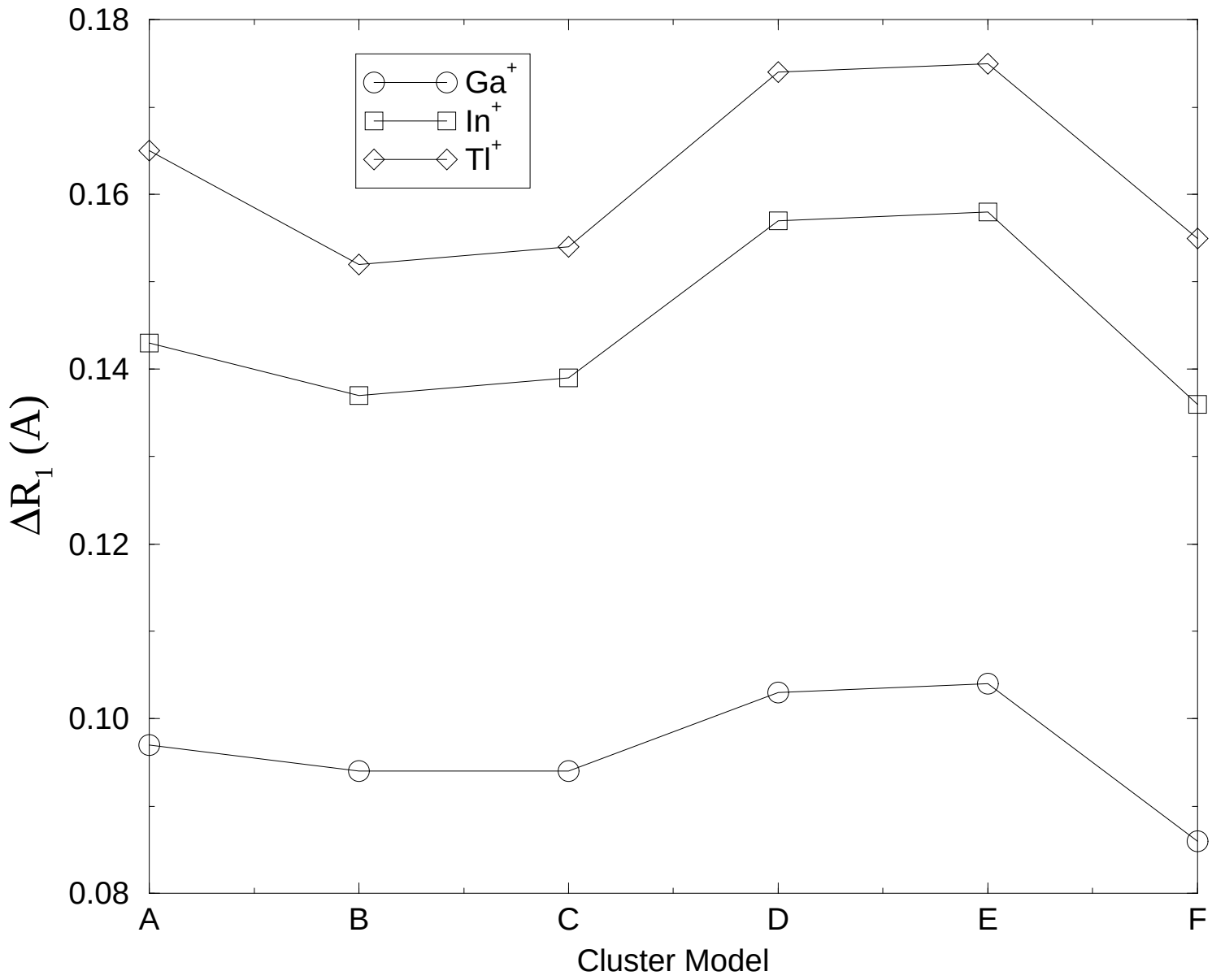
0.18
0.16
0.14
0.12
0.10
0.08
ΔR_1 (A)
A
B
C
D
E
F
Cluster Model
Ga^+
In^+
Tl^+

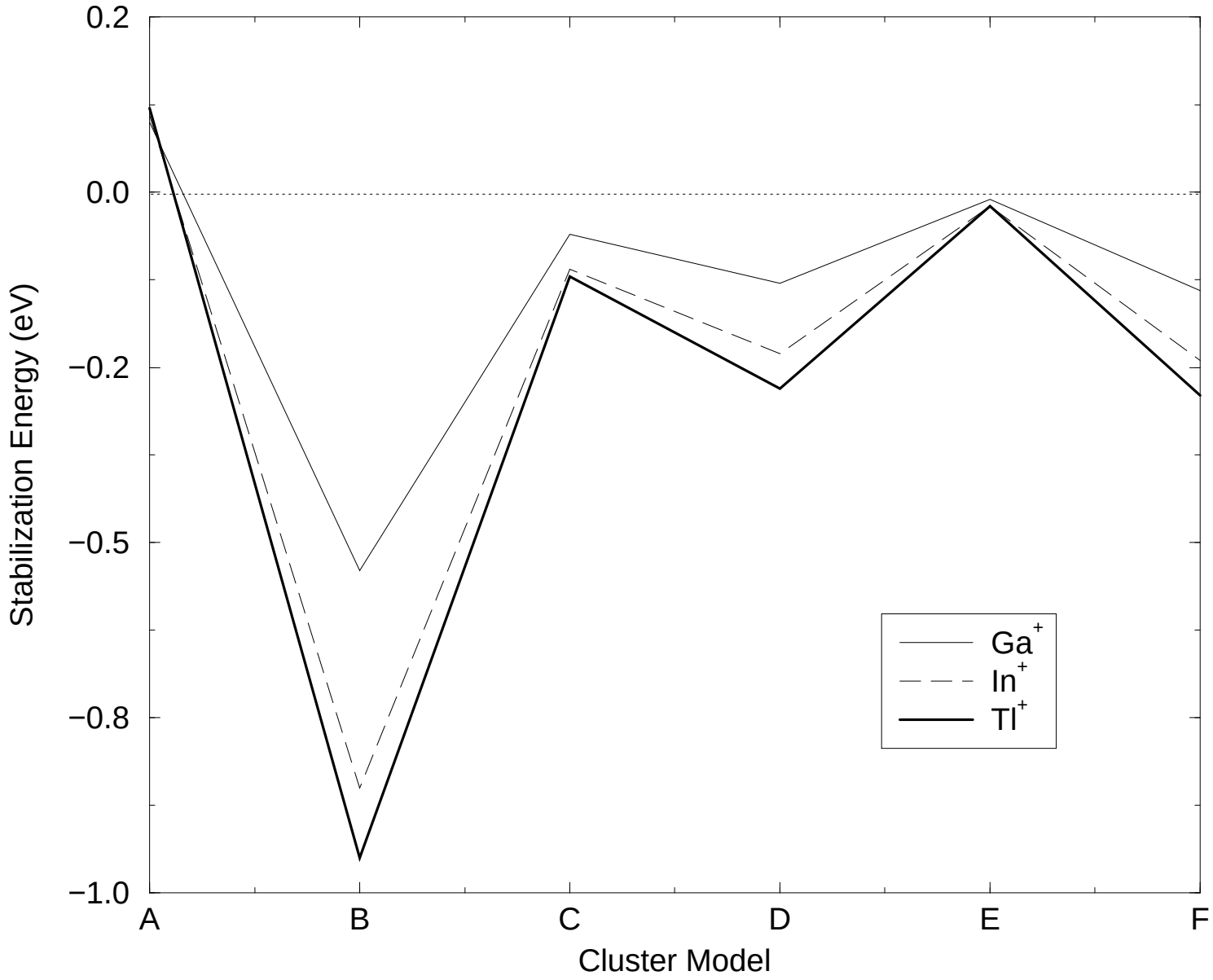
0.2
0.0
−0.2
−0.5
−0.8
−1.0
Stabilization Energy (eV)
A
B
C
D
E
F
Cluster Model
Ga+
In+
Tl+